Optical properties of α'-$Na_xV_2O_5$

M. J. Konstantinović, Z. V. Popović, and V. V. Moshchalkov
Laboratorium voor Vaste-Stoffysica en Magnetisme, Katholieke Universiteit Leuven, Celestijnenlaan 200D, B-3001 Leuven, Belgium

C. Presura
Solid State Physics Laboratory, University of Groningen, Nijenborgh 4, 9747 AG Groningen, The Netherlands

R. Gajić
Institute of Physics, P.O.Box 68, 11080 Belgrade, Yugoslavia

M. Isobe and Y. Ueda
Institute for Solid State Physics, The Univesity of Tokyo, 5-11-5 Kashiwanoha, Kashiwa, Chiba 277-8581, Japan
(Received 18 January 2002; published 28 May 2002)

The optical properties of sodium-deficient α'-$Na_xV_2O_5$ ($0.85 \leqslant x \leqslant 1.00$) single crystals are analyzed in the wide energy range, from 0.012 to 4.5 eV, using ellipsometry, infrared reflectivity, and Raman-scattering techniques. The material remains insulating up to the maximal achieved hole concentration of about 15%. In sodium-deficient samples the optical absorption peak associated to the fundamental electronic gap develops at ~ 0.44 eV. It corresponds to the transition between vanadium d_{xy} and the impurity band, which forms in the middle of the pure α'-NaV_2O_5 gap. Raman spectra measured with incident photon energy larger than 2 eV show strong resonant behavior, due to the presence of the hole-doping activated optical transitions, peaked at ~ 2.8 eV.

DOI: 10.1103/PhysRevB.65.245103 PACS number(s): 78.30.−j, 78.40.−q, 71.28.+d, 71.55.Ht

I. INTRODUCTION

α'-$Na_xV_2O_5$ belongs to the family of AV_2O_5 oxides (A = Li, Na, Ca, Mg), which have demonstrated, due to their peculiar crystal structures,[1,2] a variety of low-dimensional phenomena. The nominally pure α'-NaV_2O_5 is a mixed valence compound ($V^{4+}:V^{5+}=1:1$), with the structure consisting of vanadium-oxygen (VO_5) pyramids that are connected via common edges and corners to form layers in the (**ab**) plane. Its structure can be described as an array of parallel ladders running along the **b** axis, Fig. 1. Each rung is made of a V-O-V bond, and contains one valence electron donated by the sodium atoms, which are situated between layers. The sodium deficiency does not alter α' crystal structure[3] up to $x=0.70$, but changes the relative abundance of the V^{4+} and V^{5+} ions, e.g., introduces "extra" holes (more V^{5+} ions) in the (**ab**) planes.

α'-NaV_2O_5 is one-dimensional antifferomagnetic (AF) insulator at room temperature,[3] despite the fact that the vanadium atoms have uniform valence of $+4.5$, which indicates the quarter-filled band structure, and suggests a metallic state. However, the optical measurements[4] revealed the electronic gap of the order of 1 eV, which is formed between linear combinations of the $3d_{xy}$ states of the two vanadium ions forming the rungs.[5] The insulating ground state is argued to originate from the strong electron-electron interaction,[5,6] e.g., due to the presence of a large on-site Hubbard repulsion parameter U.

The effects of the hole doping on the optical properties of α'-NaV_2O_5 have not been studied in details. This interesting topic certainly deserves attention because of the spectacular effects observed in doped AF insulators, e.g., high-temperature superconductivity. Reduction of the Na concentration with respect to the nominally pure α'-NaV_2O_5 has a strong influence on the room-temperature Raman spectra.[7,8] The largest effect is the energy shift (about 35 cm^{-1}) of the bond-bending (V—O_3—V) 448-cm^{-1} phonon caused by the Na deficiency. Such a strong renormalization of the phonon frequency is conjectured to arise from the delocalization of the electrons from the ladder legs to the bridge oxygens.[8]

Here we further examine the electron-phonon coupling effect in α'-$Na_xV_2O_5$ by measuring Raman spectra using different laser line energies. We also analyze the influence of

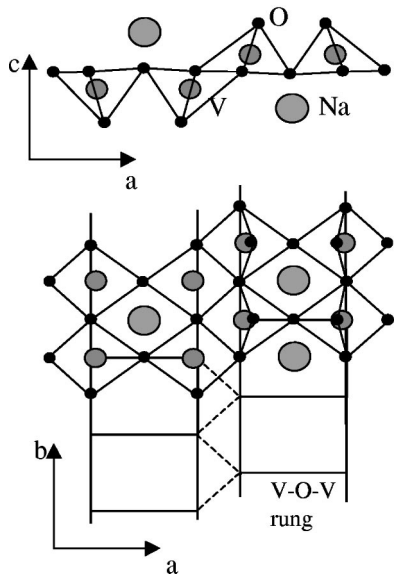

FIG. 1. Schematic representation of the α'-NaV_2O_5 crystal structure in the (001) and (010) planes. Effective representation of parallel ladders coupled in a trellis lattice is also shown.

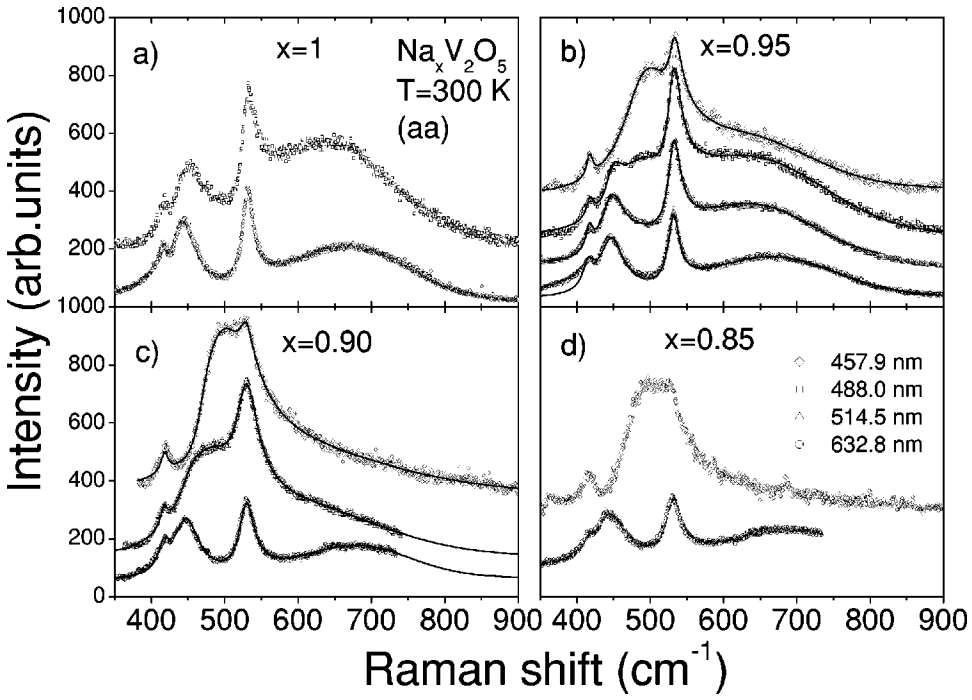

FIG. 2. Raman spectra of α'-$Na_xV_2O_5$ measured at $T=300$ K using various laser line energies for (a) $x=1$, (b) $x=0.95$, (c) $x=0.90$, and (d) $x=0.85$. The symbols are experimental data, and the fits are represented with solid lines.

the Na deficiency on the optical transitions in the mid-IR (infrared), and visible energy range. First, we show that the phonon energy renormalization is not as large as reported in Refs. 7,8, since the structure around 450–500 cm^{-1} consists in fact of two modes. Their intensity ratio changes due to the resonant conditions caused by the activation of the hole doping associated electronic band, peaked at ~ 2.8 eV. Second, we discuss the electronic structure of α'-$Na_xV_2O_5$ on the basis of the IR reflectivity and ellipsometric measurements.

II. EXPERIMENTAL DETAILS

The present work was performed on single-crystal plates of α'-$Na_xV_2O_5$ ($0.85 \leqslant x \leqslant 1.00$) with dimensions typically about $2\times4\times0.5$ mm^3 in the **a**, **b**, and **c** axes, respectively. The details of the sample preparation were published elsewhere.[2] The ellipsometric measurements were done on the (001) surfaces of the crystals, both with the plane of incidence of the light along the **a** and the **b** axes. An angle of incidence θ of 66°, was used in all experiments. Procedure for extraction of the dielectric constants is described in Ref. 9. The infrared measurements were carried out with a BOMEM DA-8 far-IR spectrometer. A DTGS pyroelectric detector was used to cover the wave-number region from 100 to 700 cm^{-1}; a liquid-nitrogen-cooled HgCdTe detector was used from 500 to 5000 cm^{-1}. Spectra were collected with 2-cm^{-1} resolution, with 1000 interferometer scans added for each spectrum. Raman spectra were measured in the backscattering configuration using micro-Raman system with DILOR triple monochromator including liquid-nitrogen-cooled charge coupled device detector. The Ar and He-Ne lasers were used as excitation sources.

III. RAMAN SPECTRA

Figure 2 shows the (aa) polarized Raman spectra of α'-$Na_xV_2O_5$, measured at room temperature, for several laser line energies. The spectra are scaled along the vertical axis for clarity. The spectra of nominally pure α'-NaV_2O_5, and the Na-deficient spectra measured with 514.5 nm laser line show the characteristic features that were already observed, and discussed in previous papers.[10–12] Here, we focus on the (350–800)-cm^{-1} energy range, where three A_g phonon modes at 418 cm^{-1}, 448 cm^{-1}, and 532 cm^{-1}, and a broad structure centered at 650 cm^{-1} are found. Two phonons at 448 cm^{-1} and 532 cm^{-1} are strongly interacting with underlying continuum, which is manifested through their asymmetric line shapes. In the Na-deficient samples this effect seems to be strongly enhanced.[8] The 448-cm^{-1} mode corresponds to the V—O_3—V bond-bending vibrations, whereas the 532-cm^{-1} mode corresponds dominantly to the bond-stretching V—O_2 vibrations with a small contribution of the V—O_3—V bond-bending vibrations.[13] The origin of the 650-cm^{-1} structure is still under debate. Its possible magnetic origin, due to the AF coupling of the electrons along the ladder direction (**b** axis), can be ruled out since the structure is observed only in the (aa) polarized configuration, and because its energy does not fit the estimates[14] of the exchange-coupling constant. The electronic band-structure calculations[15,16] show no evidence for the existence of low-lying electronic states even though both Raman and IR spectra confirmed their activity. The polaronic scenario, as discussed in Ref. 8, is also questionable since the maximum of the electron density of states does not fall above the energy of the highest frequency phonon mode. Nevertheless, Raman

TABLE I. Oscillator fit parameters (in cm^{-1}).

α'-$Na_{0.95}V_2O_5$		$\lambda=632.8$ nm	$\lambda=514.5$ nm	$\lambda=488$ nm	$\lambda=457.9$ nm
1	ω	418	418	418	418
	I	1500	1400	1200	1500
	w	12	12	12	12
2	ω_p	445	445	445	445
	I	0.5	1.8	6.5	50
	q	19	10	4.5	0.5
	Γ	20	20	20	20
3	ω		495	495	495
	I		15100	27050	46100
	w		90	80	81
4	ω_p	530	530	530	530
	I	0.7	22.7	36	17
	q	17	3.5	2.8	3.7
	Γ	10.5	10.5	10.5	10.5
5	ω	664	649	646	621
	I	27700	38100	50000	39000
	w	170	165	182	195

spectra indicate the existence of the strong electron-phonon coupling, that should be related to the charge transfer of the rung electron. The sodium deficiency introduces the holes in the rungs, so it is natural to conjecture that such charge dissonance is responsible for the bond-bending phonon renormalization.[8]

However, the Na deficiency has very little or no effect on the Raman spectra measured with the 638.2-nm line, see Fig. 2. The V—O_3—O bond-bending phonon at 448 cm^{-1} does not exhibit large energy renormalization and the 650-cm^{-1} electronic continuum is clearly visible even in the sample with the 15% hole concentration. This finding suggests that it is necessary to include the resonant effects into consideration. For example, in Fig. 2(b) we present the (aa) polarized room temperature Raman spectra of α'-$Na_{0.95}V_2O_5$ single crystal measured with several laser line energies. This graph shows a typical evolution of the Raman spectra in α'-$Na_xV_2O_5$ under strong resonant conditions. Thus, we fit the Raman spectra using Fano model,[17] which includes the effects of the interaction between discrete (phonon) and continuum (electron) states. For a particular energy range, $350-800$ cm^{-1}, we took five oscillators with 17 parameters. It is important to note, as it will be evident from our fits, that not all the parameters are crucial for the observed line-shape change. The parameters of the first Lorentz oscillator at 418 cm^{-1} are kept constant, and used for the normalization of the spectra, since this mode does not show any change of intensity, energy, or half width under resonant conditions. For the phonons at 448 cm^{-1} and 532 cm^{-1} we adopt the Fano line shapes of the form[17] $I\sim(q+\epsilon)^2/(1+\epsilon^2)$, with q being the ratio of the Raman tensors for discrete vibronic and continuum electronic scattering. The parameter ϵ is $(\omega-\omega_p)/\Gamma$, where ω_p and Γ represent the real and the imaginary part of the phonon selfenergy, when its interaction with a continuum is taken into account. The continuum is represented with a Gaussian. The fifth oscillator appears at about 495 cm^{-1} and its difference from the 448-cm^{-1} mode is seen in the Raman spectra of α'-$Na_{0.95}V_2O_5$, measured with 488-nm laser line, see Fig. 2(b). It is difficult to argue whether 495-cm^{-1} mode interacts with the continuum or not, so we used Lorentzian for this mode. The results of the fit are shown as solid lines in Fig. 2. The fits are excellent in all cases. The values of the parameters for α'-$Na_{0.95}V_2O_5$ are presented in the Table I.

The major change in Raman spectra under resonant conditions is described by only four parameters; intensity (I) and q, of the 448-cm^{-1} mode, intensity of the 495-cm^{-1} mode, and the ω of the Gaussian. The values of the Γ and $\omega_p=\omega_M-\Gamma/q$ (ω_M is the position of the mode maximum) obtained from these fits are, within experimental error, the same for all spectra. Since the Γ is squared matrix element of the coupling between continuum and discrete state, this parameter should have no relationship with scattering wavelength.[15] This is to be expected for the pure resonant effect, unless there is a change in the strength of the electron-phonon interaction, caused by the sodium deficiency. However, these parameters are also found to be the same for all samples with different Na concentrations, which indicates that the electron-phonon interaction is not dependent on the hole concentration. The parameter q of the 448-cm^{-1} mode has a strong dependence on scattering frequency, and its variation increases with increasing sodium deficiency. Similar increase is also found for the intensity of the 495-cm^{-1} mode. The square of the parameter q represents the ratio of the scattering probability for discrete state to that of the continuum, hence q can exhibit a dependence on the scattering frequency if the two processes have different frequency dependencies. This is confirmed by our fits. The new mode at about 495 cm^{-1} is probably bond-bending vibration of the rung without electron, since its energy is close to the corresponding bond-bending vibration in V_2O_5 (482 cm^{-1}, Ref. 18). Under resonance the change of these parameters (more precisely $1/q$, and/or intensity) can be related to the change of the optical conductivity or dielectric constant.[19] In the nominally pure α'-NaV_2O_5, there is no electronic band in the visible energy region,[4,20] and the Raman spectra show no dramatic transformation induced by the measurements with different laser line energies. However, strong resonant scattering in the Na-deficient samples should originate from the new electronic transitions at energies between 2 and 3 eV. This band, induced by hole doping is found at about 2.8 eV using ellipsometric measurements, as discussed in the following section.

IV. ELLIPSOMETRIC AND INFRARED MEASUREMENTS

The optical conductivity of α'-$Na_xV_2O_5$, obtained from the ellipsometric measurements is given in Fig. 3. For the nominally pure α'-NaV_2O_5 the bands at the energies 0.9, 1.2, and 3.2 eV for σ_a, and at 1.2, 1.6, and 3.7 eV for σ_b are found in accordance with previous papers.[20–23] The sodium deficiency causes the activation of the new optical transitions at about 2.8 eV in σ_a and at 3.2 eV in σ_b, see Fig. 3. As we have already mentioned, the 2.8-eV peak is responsible for

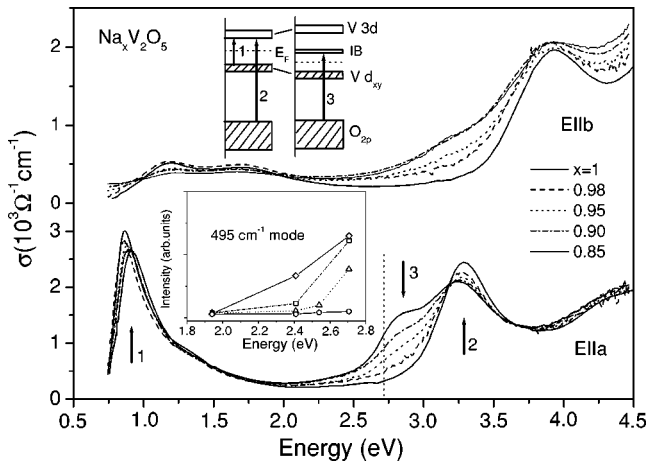

FIG. 3. Optical conductivity of α'-$Na_xV_2O_5$ measured at $T=300$ K for $E\|a$ (lower panel) and $E\|b$ (top panel). The $x=1$ (solid), $x=0.98$ (dashed), $x=0.95$ (dot), $x=0.90$ (dash-dot), and $x=0.85$ (solid). Vertical dotted line is placed at energy that denotes the highest laser energy used in Raman experiment. Low inset: Intensity of 495 cm^{-1} mode as a function of the laser line energy for various x. Top inset: Schematic representation of the electronic levels in α'-$Na_xV_2O_5$.

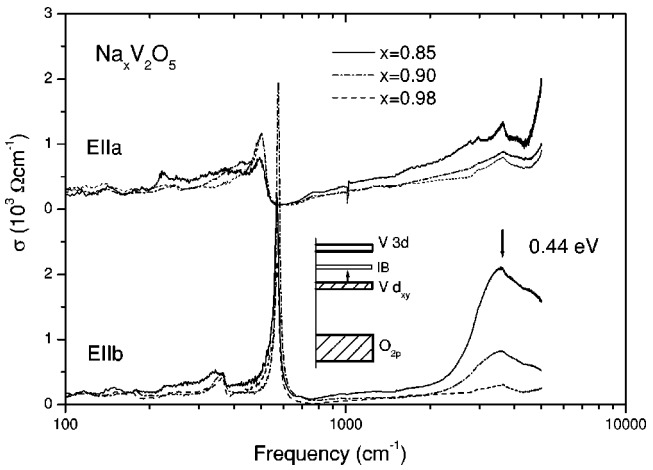

FIG. 4. Optical conductivity of α'-$Na_xV_2O_5$ obtained from the Kramers-Kronig analysis of the reflectivity spectra in $E\|a$ (top panel) polarizations, and $E\|b$ (lower panel). Inset: Schematic representation of the V3$d_{x,y}$-IB transitions.

the resonant behavior of the (aa) polarized Raman spectra. The intensity of the 495-cm^{-1} mode, see inset Fig. 3, and the parameter q^{-1} of the 448-cm^{-1} phonon, mimic the change in σ_a, which reinforces our conclusions about resonant effects in the Raman spectra.

The essential features of the α'-NaV_2O_5 electronic structure are formed from oxygen $2p$ and vanadium $3d$ states. The fully occupied oxygen $2p$ states are located about 3 eV below the lowest of the V3d states split by ligand field.[24] The lowest state of the $V^{4+}3d$ manifold, $3d_{xy}$ state, is occupied by one electron. The V-O-V rung is formed through the electron hopping via oxygen O_3 states. Due to this coupling, usually denoted as t_a, two $3d_{xy}$ orbital levels form symmetric and antisymmetric combinations of levels (bonding and antibonding levels) that are split by $2t_a \sim 0.7$ eV.[16] The insulating state appears due to the large on-site Hubbard repulsion U which pushes the Fermi level in the middle of the gap between bonding and antibonding states.[5,6] Thus, the main peak in the optical spectrum along the **a** direction at 0.9 eV seems to originate from the transitions between bonding and antibonding states of the same rung.[9] The higher energy bands, above 3 eV, are similar to those found in V_2O_5,[25] and correspond to the O2p-V3d type of transitions.

The sodium deficiency changes the relative abundance of the V^{4+} and V^{5+} ions. In fact, introduction of holes leeds to the formation of rungs without electrons, similar to the V^{5+}—O_3—V^{5+} bonds in V_2O_5. Therefore, the optical transitions above 2 eV should also be similar in V_2O_5 and α'-$Na_xV_2O_5$. However, previous studies[20–23] did not clearly show what kind of the final state is involved in the 3.2-eV (σ_a) transition, and this turns out to be the most important information in order to understand the electronic structure of the Na-deficient samples. If the final state is the bonding V3d_{xy} state, as described in Ref. 23 the α'-NaV_2O_5 should be in the metallic state, which is in strong disagreement with the observed insulating behavior. In the insulating state, the optical transitions between O2p and the bonding V3d_{xy} states should be forbidden. The next possibility is that the final state of 3.2-eV peak corresponds to the nonbonding V $3d_{xy}$ state, which forms when there are two electrons in the rung. According to the modified Heitler-London model, proposed in order to account for the observed features in the optical conductivity spectra of α'-NaV_2O_5,[9] the nonbonding band lies in the middle of the bonding-antibonding gap. The sodium deficiency is expected to drive the Fermi level inside of the bonding bend, which now activates the transitions between the O2p and bonding V3d_{xy} states. In this case, the bonding level is partially filled, so this scenario also relies on the formation of the metallic state in α'-$Na_xV_2O_5$, which is not observed.

The IR reflectivity measurements show that the material remains insulating up to the maximal achieved hole concentration of about 15%. The optical conductivity, obtained from the Kramers-Kronig analysis of the IR reflectivity, is presented in Fig. 4. In both σ_a and σ_b spectra of α'-$Na_xV_2O_5$ we found no Drude behavior at low frequencies. Instead, the dominant feature activated by the Na deficiency is observed in σ_b at about 0.44 eV, with a half width at half maximum of about 0.25 eV. Note that its energy corresponds to the half of the energy of 0.9-eV peak.

Clearly, all scenarios discussed so far are not yet adequate to fully describe the optical transitions and the electronic structure of the α'-$Na_xV_2O_5$. We argue below that the electronic structure based on the four electronic bands can account for the major features observed in the optical conductivity of α'-$Na_xV_2O_5$. Simplified schematic representation of the optical transitions, and the energy levels in α'-NaV_2O_5, is shown in the inset of Fig. 3. In the nominally pure α'-NaV_2O_5, the arrows in the left side of the inset of Fig. 3 represent the optical transitions which we have already discussed. The energy levels of the sodium deficient samples are shown in the right side of the inset of Fig. 3. In order to account for the appearance of the new modes at 2.8 eV and

0.44 eV in α'-$Na_xV_2O_5$ spectra, we have to assume the existence of the impurity band (IB), which forms inside the electronic gap of the pure α'-NaV_2O_5. This band is further on considered to be empty, so the optical transitions, denoted as processes "3" in Fig. 3, may appear in the spectra. We find strong support for our assumption in the electronic structure, and the optical spectra[25] of V_2O_5. In this compound very narrow electronic band, which is separated from the rest of the conduction band by an additional gap, exists at the energy of about 2.5 eV. Thus, it is possible that impurity band in sodium-deficient samples has its origin from this level. If so, the optical process "3" corresponds to the transition between oxygen 2p band and IB. Its energy, $E_3=E_2-1/2E_1\sim 2.8$ eV, indicates that the IB forms almost exactly in the middle of the electronic gap of the pure α'-NaV_2O_5. This is further supported by the existence of the mid-IR absorption peak at about $E_{IB}=1/2E_1\sim 0.44$ eV, see Fig. 4, which corresponds to the transitions between V d_{xy} and IB states. The nature of the IB determines the electronic properties of α'-$Na_xV_2O_5$. By increasing sodium deficiency the 0.44-eV peak grows in intensity and its width increases, which indicates that the IB gains dispersion. In order to preserve the preferential insulating ground state (at least up to 15% deficiency) this process is accompanied with the increase of the gap between vanadium $3d$ bands. This is evident from the energy increase of the peak "1" in σ_a. Because of that, and since this band is indeed very narrow (0.25 eV), IB does not overlap with the occupied d_{xy} band, and the solution is an insulator since the Fermi level is placed in the middle of the gap between bonding d_{xy} states and IB. The 0.44-eV peak is found to be much stronger in σ_b then in σ_a spectra. Thus, we tentatively assigned it as the inter-rung electron transition along the **b** axis.

V. CONCLUSION

In conclusion, we present the analysis of the optical properties of α'-$Na_xV_2O_5$ using ellipsometric, IR and Raman-scattering techniques. Despite strong hole doping the material remains insulating up to the doping concentration of about 15%. The insulating state appears as a consequence of very narrow impurity band formed in the middle of the electronic gap of the pure α'-NaV_2O_5. The optical absorption peak develops at ~ 0.44 eV and corresponds to the transitions between vanadium V d_{xy} and impurity band states. The change of the Raman-active multiple phonon structure upon doping, in the energy range between 450 and 550 cm^{-1}, is the consequence of the resonance, and is caused by the activation of the hole doping associated optical transitions peaked at about 2.8 eV .

ACKNOWLEDGMENTS

M.J.K. and Z.V.P. acknowledge support from the Research Council of the K.U. Leuven and DWTC. The work at the K.U. Leuven is supported by Belgian IUAP and Flemish FWO and GOA Programs.

[1] M. Isobe, Y. Ueda, J. Magn. Magn. Mater. **177-181**, 671 (1998).
[2] M. Isobe and Y. Ueda, J. Alloys Compd. **262-263**, 180 (1997).
[3] M. Isobe and Y. Ueda, J. Phys. Soc. Jpn. **65**, 1178 (1996).
[4] S.A. Golubchik, M. Isobe, A.N. Ivlev, B.N. Mavrin, M.N. Popova, A.B. Sushkov, Y. Ueda, and V.N. Vasil'ev, J. Phys. Soc. Jpn. **66**, 4042 (1997).
[5] H. Smolinski, C. Gros, W. Weber, U. Peuchert, G. Roth, M. Weiden, and C. Geibel, Phys. Rev. Lett. **80**, 5164 (1998).
[6] V.A. Ivanov, Z.V. Popović, O.P. Khuong, and V.V. Moshchalkov, Europhys. Lett. **56**, 74 (2001).
[7] M.N. Popova, A.B. Sushkov, S.A. Golubchik, B.N. Mavrin, V.N. Denisov, B.Z. Malkin, A.I. Iskhakova, M. Isobe, and Y. Ueda, Zh. Éksp. Teor. Fiz. **115**, 2170 (1999) [JETP **88**, 1186 (1999)].
[8] W.S. Bacsa, R. Lewandowska, A. Zwick, and P. Millet, Phys. Rev. B **61**, 14 885 (2000).
[9] C. Presura, D. van der Marel, M. Dischner, C. Geibel, and R.K. Kremer, Phys. Rev. B **62**, 16 522 (2000).
[10] M. Weiden, R. Hauptmann, C. Geibel, F. Steglich, M. Fischer, P. Lemmens, and G. Güntherodt, Z. Phys. B: Condens. Matter **103**, 1 (1997).
[11] Z.V. Popović, M.J. Konstantinović, R. Gajić, V. Popov, Y.S. Raptis, A.N. Vasil'ev, M. Isobe, and Y. Ueda, J. Phys.: Condens. Matter **10**, L513 (1998).
[12] H. Kuroe, H. Seto, J. Sasaki, T. Sekine, M. Isobe, and Y. Ueda, J. Phys. Soc. Jpn. **67**, 2881 (1998).
[13] Z.V. Popović, M.J. Konstantinović, R. Gajić, V. Popov, Y.S. Raptis, A.N. Vasil'ev, M. Isobe, and Y. Ueda, Solid State Commun. **110**, 381 (1999).
[14] B. Grenier, O. Cepas, L.P. Regnault, J.E. Lorenzo, T. Ziman, J.P. Boucher, A. Hiess, T. Chatterji, J. Jegoudez, and A. Revcolevschi, Phys. Rev. Lett. **86**, 5966 (2001).
[15] H. Seo and H. Fukujama, J. Phys. Soc. Jpn. **67**, 2602 (1998).
[16] M. Cuoco, P. Horsch, and F. Mack, Phys. Rev. B **60**, R8438 (1999).
[17] U. Fano, Phys. Rev. **124**, 1866 (1961).
[18] P. Clauws, J. Broeckx, and J. Vennik, Phys. Status Solidi B **131**, 459 (1985).
[19] F. Cardeira, T.A. Fjeldly, and M. Cardona, Phys. Rev. B **8**, 4734 (1973).
[20] A. Damascelli, D. van der Marel, M. Gruninger, C. Presura, T.T.M. Palstra, J. Jegoudez, and A. Revcolevschi, Phys. Rev. Lett. **81**, 918 (1998).
[21] M.J. Konstantinović, J. Dong, M.E. Ziaei, B.P. Clayman, J.C. Irwin, K. Yakushi, M. Isobe, and Y. Ueda, Phys. Rev. B **63**, 121102 (2001).
[22] V.C. Long, Z. Zhu, J.L. Musfeldt, X. Wei, H.-J. Koo, M.-H. Whangbo, J. Jegoudez, and A. Revcolevschi, Phys. Rev. B **60**, 15 721 (1999).
[23] S. Atzkern, M. Knupfer, M.S. Golden, J. Fink, A.N. Yaresko, V.N. Antonov, A. Hübsch, C. Waidacher, K.W. Becker, W. von der Linden, G. Obermeier, and S. Horn, Phys. Rev. B **63**, 165113 (2001).
[24] K. Kobayashi, T. Mizokawa, A. Fujimori, M. Isobe, and Y. Ueda, Phys. Rev. Lett. **80**, 3121 (1998).
[25] V.G. Mokerov, V.L. Makarov, V.B. Tulvinskii, and A.R. Begishev, Opt. Spectrosc. **40**, 58 (1976).